

# Lagrangian tracking of soot particles in LES of gas turbines

Lucien Gallen<sup>a,\*</sup>, Anne Felden<sup>a</sup>, Eleonore Riber<sup>a</sup>, Bénédicte Cuenot<sup>a</sup>

<sup>a</sup>*CERFACS, 42 avenue Gaspard Coriolis, 31047 Toulouse, France*

---

- **Colloquium:** Gas Turbine and Rocket Engine Combustion
- **Paper length:** Method 1 is used. Total length = 6094 words: main text 3566 words, references 681 words, captions 259 words, figures 1323 words (Fig 1 = 95 words, Fig 2 = 85 words, Fig 3 = 396 words, Fig 4 = 121 words, Fig 5 = 152 words, Fig 6 = 474 words), tables 121 words (Tab.1 = 38 words, Tab.2 = 38 words, Tab.3 = 45 words), equations 144 words
- **Supplemental Material:** No
- **Reproduction of color figures:** All figures to be printed in grey.

## Abstract

Expected stringent legislation on particulate matter (PM) emission by gas turbine combustors is currently motivating considerable efforts to better understand, model and predict soot formation. This complex phenomenon is very difficult to study in detail with experiment, and numerical simulation is an essential complementary tool. Considering that the chemistry of

---

\*Corresponding author:

*Email address:* [gallen@cerfacs.fr](mailto:gallen@cerfacs.fr) (Lucien Gallen)

soot particles strongly depends on their size, the numerical prediction of soot formation requires the description of their size distribution. To do so, either Eulerian methods (sectional or moments), or stochastic Lagrangian approaches are reported in the literature. In the present work a far more simple semi-deterministic Lagrangian approach is proposed. Combined to the semi-empirical model of Leung *et al.* (1991) for soot chemistry, the Lagrangian approach is first validated on a one-dimensional premixed ethylene-air flame. The model is then applied to a gaseous non-premixed ethylene-air burner measured at DLR and computed with Large Eddy Simulation (LES). The gaseous chemistry is described with an Analytically Reduced Chemistry (ARC) to guarantee a good prediction of combustion and gaseous soot precursors. Results are validated against experiment and compared, in terms of accuracy and CPU cost, to an Eulerian semi-empirical model. To the authors knowledge, it is the first time that such Lagrangian particle tracking approach is used for soot. Results obtained in terms of accuracy and computing time are very encouraging.

*Keywords:*

Soot particles, Lagrangian tracking, Large Eddy Simulation, Gas Turbine

---

## 1. Introduction

Particulate Matter (PM) emitted from practical combustion devices contribute to air pollution, which has a strong negative impact on the population health [1] and air quality. This includes soot, which results from a complex gaseous and heterogeneous chemical process. When emitted at high altitude, soot increases significantly the local concentration of aerosols in the atmosphere inducing a possible artificial radiative forcing via the formation of contrails. On the ground, emitted soot particles can be inhaled and, depending on their size, penetrate more or less deeply in the human body where it can trigger specific diseases. In this context, the design of the next generation of combustor devices with limited soot emission has become a major challenge for engine manufacturers. To do so numerical simulation is an essential tool which, if sufficiently accurate, allows a better understanding and control of soot formation.

Soot particle size is not only critical for their toxicity, but also for their formation / destruction processes, as these involve heterogeneous chemistry at the particle surface. The prediction of soot particle formation therefore requires to describe their size distribution. A population of soot particles is then represented by its local and instantaneous Number Density Function (NDF), defined as the number of particles of a given size. The NDF is often bimodal due to the constant inception of very small soot particles and the final large aggregates resulting from successive collisions and surface reactions [2]. The NDF is the solution of the Population Balance Equation (PBE), which is solved using statistical approaches. Three classes of resolution methods of the PBE are commonly used: the Method of Moments

(MOM), the Sectional Method (SM), and the Monte Carlo (MC) stochastic Lagrangian approach. The MOM aims at calculating a set of statistical moments of the NDF [3–6], while SM [7–9] and MC directly solve the PBE to obtain the NDF. Although they have allowed to obtain very good results [10, 11], these methods are complex, demand specific numerics and are computationally expensive.

An alternative is proposed in the present work, based on a simple semi-deterministic Lagrangian approach. The method is deterministic in the sense that physical particles are tracked, contrary to MC dealing with stochastic particles. It however still includes stochastic processes such as collisions. To limit the computational time, only a subset of particles is computed, representative of all particles possibly present in a control volume. With this strategy, Lagrangian particle tracking becomes affordable in real complex geometries such as aircraft or internal engines. The choice of such a Lagrangian formalism for nano-particles is still on the fringes of the official methods. The reason is to be found in the prohibitive computational cost of the Lagrangian tracking of all physical particles in a 3D complex configuration. As a consequence, most Lagrangian calculations are restricted to the resolution of realizability issues in MOM [12]. An attempt of deterministic Lagrangian calculation of soot has been made very recently by Ong et al. [13] where however the interactions between particles were neglected. This considerably simplified the implementation but also significantly reduced the accuracy as particle interactions are essential. Today, both the progress made in parallel computing and the semi-deterministic Lagrangian concept allow to overcome this computational cost issue, as will be demonstrated in the

present paper. This requires however an optimum parallel efficiency of the Lagrangian solver, as well as a careful control of statistical convergence.

In the following, the derivation of the semi-deterministic Lagrangian method is explained in details. Combined to a semi-empirical model for soot evolution [14], it is then validated in a one-dimensional sooting premixed flame. Finally, an experimental gaseous ethylene-air non-premixed burner [15] already investigated with LES and a one-section SM approach [16, 17] is used to assess the computational cost and accuracy provided by the new Lagrangian method.

## 2. Soot modeling

### 2.1. Lagrangian formalism

The present methodology is based on the Discrete Particle Simulation (DPS), similar to what is used for spray computations. Contrary to dilute sprays, soot particle populations are dense, so that collisions have a high probability and must be accounted for. Indeed, they play an essential role in the soot particles size distribution. The proposed approach, so-called EL POLY, relies on the following assumptions:

- **Dynamics:** soot particles are tracers. This means that neither drag nor thermophoresis effects are taken into account. Considering that soot are mostly nanometric and evolve in highly turbulent flows (low Stokes number), this assumption seems reasonable.
- **Temperature:** Soot particle temperature is homogeneous and equal

to the surrounding gas temperature. This assumption is also justified by the nanometric size of the particles.

- **Shape:** The particles are spherical. This is clearly a very strong assumption that is not true in most cases, but is done here as a first step for the demonstration of the new Lagrangian approach. It will be shown that this approach is a good framework to relax this assumption in future work.

In the DPS approach, particles are handled as point sources, having properties like temperature, size, velocity, surface area, collision diameter, etc. just as in stochastic methods [10]. In particular the spherical assumption can be easily relaxed through the particle surface or a joint surface-volume model [18]. In addition, as only a subset of physical particles are computed in the semi-deterministic concept, each particle also has a weight  $w_k$  (also denoted *rparcel*) representing the number of physical particles having the same properties at the same location and time. Being not constant nor uniform, this *rparcel* is not a user-defined parameter, but varies for each particle and results from the control of statistical convergence. The objective is to describe with sufficient accuracy the NDF in each control volume (mesh cell), given a maximum allowed number of computed particles per control volume  $N_{soot}^{max}$ . To do so, at each time step, particles grouping is revisited via conservative merging operations based on criteria of properties proximity (size, location). This merging process will be described in Sec. 2.3.

## 2.2. The Leung model

The chosen soot model is the semi-empirical, two-equations Leung model [14], employed in many previous studies [16, 17, 19]. The model describes soot as a monodisperse particle size distribution population, and was written in both Eulerian and Lagrangian formulations. Although this model is too simple to be quantitatively accurate, this choice was made to ease the comparison between Eulerian and Lagrangian approaches, which is the main objective of this paper.

In the Leung model, the soot particle mass evolves as:

$$\frac{dm_p}{dt} = \frac{\dot{\omega}_s}{N} - \frac{m_p}{N} \dot{\omega}_n N_A \left[ \frac{kg}{s} \right] \quad (1)$$

where  $N$  is the soot particle number density per volume,  $N_A$  is the Avogadro number and  $m_p$  is the particle mass.  $\dot{\omega}_n$  and  $\dot{\omega}_s$  refer to soot number density and mass fraction source terms, and are detailed later in this Section. Note that condensation is not taken into account. The monodisperse approach has been validated [17] in non-premixed laminar ethylene-air flames studied experimentally by [20] and often used for soot modeling validation. The gas-phase chemistry was described by an Analytically Reduced Chemistry including 29 species, among which 11 were set in Quasi Steady State [17]. The reaction rate constants of the Leung model have been calibrated in order to improve soot prediction. This is a standard procedure for such simple model, that has anyway a limited accuracy. It is however not the objective here to demonstrate the validity of the Leung model, but rather to guarantee a correct behavior before focusing on the soot numerical formalism.

The source terms of the Leung model are now detailed.

### 2.2.1. Nucleation

Nucleation processes characterize the inception of the nascent soot particles (nuclei). The corresponding source term reads:

$$\dot{\omega}_{n,nu} = \frac{R_{nu}}{N} \left( M_s - m_{p,nu} N_A \frac{2}{C_{min}} \right) \quad (2)$$

where  $\dot{\omega}_{n,nu}$  is the nucleation part of the source term  $\dot{\omega}_n$ ,  $M_s$  is the soot molecular weight,  $C_{min}$  is a constant, and  $R_{nu}$  is the nucleation reaction rate defined by Leung et al. [14]:

$$R_{nu} = k_{nu}(T) [C_2H_2] \quad (3)$$

where  $k$  refers to the reaction rate (from [17]),  $T$  is the gas temperature, and  $[-]$  stands for molar concentration. As the Lagrangian formalism is based on discrete particles, a new particle is created only after the nucleation source term is found sufficiently large. The new particle then has an initial weight equal to the number of generated nuclei, and is injected at a random position in the control volume with a given initial diameter. This initial diameter can be retrieved analytically from Eq. 2, considering that nuclei are formed at the end of the nucleation process, i.e.,  $\dot{\omega}_{n,nu} = 0$ . This gives an initial value of 0.98 nm, which will be used in all simulations presented in this paper.

In the current model, nucleation contributes only to the inception of soot particles and does not modify their properties. Therefore it does not contribute to the source term  $\dot{\omega}_s$ .

### 2.2.2. Surface reactions

Surface reactions act on the soot mass fraction source term  $\dot{\omega}_s$  in Eq. 1 with two contributions :

$$\dot{\omega}_s = \dot{\omega}_{s,sg} - \dot{\omega}_{s,ox} \left[ \frac{kg}{m^3s} \right] \quad (4)$$

where subscripts  $_{sg}$  and  $_{ox}$  refer to surface growth and oxidation, and respectively read :

$$\dot{\omega}_{s,sg} = k_{sg}(T) [C_2H_2] S^{1/2} M_s \quad (5)$$

$$\dot{\omega}_{s,ox} = (k_{ox,O_2}(T) [O_2] + k_{ox,OH}(T) X_{OH}) S M_s \quad (6)$$

where  $X_{OH}$  refers to the molar fraction of OH species. Surface reactions are directly linked to the soot surface area per unit volume  $S = \pi/4 d_p^2 N$ , if spherical particles of diameter  $d_p$  are assumed.

### 2.2.3. Coagulation

For a monodisperse size distribution of soot particles, the coagulation source term reduces to the same global source term for all particles. Polydisperse coagulation is more complex and has been widely investigated for particles and aerosols [21–23]. Usually stochastic approaches are used. In the present approach, the deterministic Lagrangian tracking of a subset of physical particles does not allow to realize all possible coagulation events and a probability of coagulation is introduced. Coagulation events are then computed according to this probability. Following Kruis et al. [24], we start from binary collisions. Considering a particle pair  $(i,j)$  with  $i \neq j$ ,  $\beta_{i,j}$  (called coagulation kernel) describes the collision rate between both particles. For symmetry reasons  $\beta_{i,j} = \beta_{j,i}$  and the total coagulation rate between all particles represented by the pair  $(i,j)$  is  $\beta_{i,j}^* = \max(\omega_i, \omega_j) \beta_{i,j} / v$ , with  $v$  the

control volume. The coagulation kernel is calculated in the free molecular regime as in the original Leung model:

$$\beta_{i,j} = C_a \sqrt{\frac{\pi \kappa T}{2 \rho_s}} \left( \frac{1}{v_i} + \frac{1}{v_j} \right)^{\frac{1}{2}} (d_{p,i} + d_{p,j})^2 \left[ \frac{m^3}{s} \right] \quad (7)$$

where  $C_a$  is the agglomeration rate constant equal to 9.0 higher than the commonly used value around 2.0 [9],  $\kappa$  is the Boltzmann constant, and  $\rho_s$  is the soot density equal to 2000 [ $kg \cdot m^{-3}$ ]. The free molecular regime assumption considers that the two particles of volume  $v_i$  and  $v_j$  have a size much smaller than the mean free path in the gas. The probability of coagulation for each pair of particles  $(i, j)$  is then  $P_{i,j} = \beta_{i,j}^* / \sum_{k,l} \beta_{k,l}^*$ .

This probability is used in the Lagrangian tracking approach as follows:

1. At the cell level,  $\beta_{i,j}^*$  is computed for each pair of particles  $(i, j)$ , and the maximum coagulation rate in the cell  $\beta_{max}^*$  is determined.
2. The acceptance-rejection method [25] is applied: selecting a pair of soot particles  $(i, j)$ , coagulation occurs if  $r \leq \beta_{i,j}^* / \beta_{max}^*$ , where  $r \in [0, 1]$  is a random number. Otherwise, the selected pair does not coagulate, and the operation is repeated until one coagulating pair is found [26].
3. The selected coagulation event is realized according to the constant-number method [26].
4. The coagulation time step is computed as the inverse of the sum of all coagulation rates :  $\tau_{coa} = 1 / \sum_{i,j} \beta_{i,j}^*$  [24, 27], and an event-driven coagulation process is applied: as soon as one coagulation event takes place, a waiting time  $\tau_{coa}$  is set before the next coagulation event.

The above coagulation model assumes that the particles in the control volume are sufficiently numerous, and describe a sufficient number of discrete states

of particles to fully describe coagulation statistics.

### 2.3. Control of statistical convergence

Lagrangian approaches require a minimum number of particles to reach statistical convergence. On the other hand, the inception of nascent soot particles implies the constant creation of new particles in the control volume, increasing their number in an uncontrolled way. In MC simulations, resizing [28] or constant-number approaches [29] are applied to nucleation [30]. In the present Lagrangian formulation, the constant-number approach is retained. This implies defining a maximum number of particles, sufficient to reach statistical convergence, and merging of weighted particles to keep their number below the maximum, as was already used in [2]. Particles can be removed randomly [21, 30, 31] but in order to enhance statistical convergence, it is more efficient to merge particles with close enough properties (size here) [26]. To do so, particles and their weights are controlled as follows:

- **Maximum number of particles:** A constant threshold value  $N_{soot}^{max}$  is applied to control the number of computed particles which are merged if  $N > N_{soot}^{max}$ .
- **Particle creation:** The nascent particles are created with a weight dictated by both the control volume and the numerical timestep to guarantee a number of particles below  $N_{soot}^{max}$ .
- **Merging:** Particle merging is controlled by a criterion based on their position and diameter.

### 3. Validation in laminar flames

The Lagrangian polydisperse methodology (EL POLY) was implemented in the code AVBP jointly developed by CERFACS and IFPEN. To benefit from the difference between the compressible flow timestep controlled by acoustics, and the particle motion convective timestep which is much larger, Lagrangian iterations are performed only after a number  $f_s$  (soot frequency) of flow iterations. This leads to a significant gain of computational cost without losing accuracy, as illustrated in Table 1 showing the contribution of the Lagrangian solver to the total computational time for different values of  $f_s$ . The value of the soot frequency  $f_s$  depends on the case and the numerical setup, and can be estimated as  $f_s = \alpha \tau_{min} / \tau_f$ , where  $\tau_f$  is a flow time scale and  $\tau_{min}$  corresponds to the minimum characteristic time of soot processes among nucleation, surface reactions and coagulation. The coefficient  $\alpha$  allows to filter out some unsteadiness of the flow and depends on the application. In the present case  $\alpha = 2$ . Note that the soot frequency has to be chosen carefully to guarantee a maximum gain in computational cost and a minimum error.

To assess the quality of the proposed method applied to gas turbines, the pressurised 1D premixed ethylene/air sooting flame from the International Sooting Flame workshop (ISF Target Flame 4 : Laminar Premixed Pressurised 2 [32]) is first computed. The equivalence ratio is high:  $\phi = 2.3$  ( $C/O = 0.766$ ), and the pressure is 3 bars. For this flame  $f_s$  is estimated at 5, for which the error is still found negligible (See Table 1). Higher values lead to significantly higher errors.

Soot frequency, $f_s$	1	5	10	20
Lagrangian solver, %	25	9	6	4
Maximum Error, %	0	3.3	18	37

Table 1: Contribution of the Lagrangian solver to the computational time for different values of  $f_s$  and maximum relative error on soot prediction for the ISF Target Flame 4.

For this case  $N_{soot}^{max}$  is set to 20 per control volume. Soot has been computed with both the monodisperse (in both Eulerian (EE) and Lagrangian (EL MONO) formulations) and polydisperse (EL POLY) approach. For EL MONO, the soot particle mass is governed by Eq. 1, the nuclei diameter is set to the mean diameter and the coagulation is based on Eq. 7 where particles have the same diameter. Results are compared in Fig. 1. As expected EE

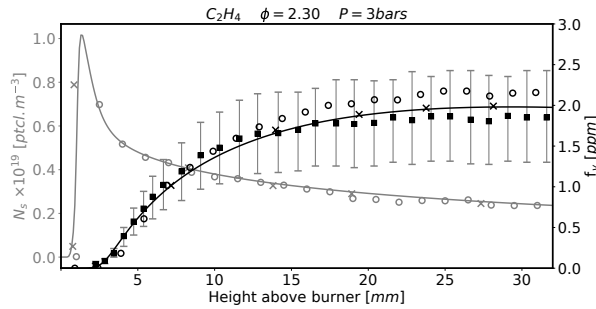


Figure 1: Soot number density (left axis, grey line) and soot volume fraction (right axis, black line) in the ISF Target Flame 4 (Laminar Premixed Pressurised 2). Comparison between experiment [32] (squares),

EE (lines), EL MONO (crosses) and EL POLY (circles).

and EL MONO are strictly identical and reproduce well the experiment as in [17]. The EL POLY approach gives also the same soot number density, but a slightly higher soot volume fraction downstream the flame.

To go further, the same 1D sooting flame is computed without surface reactions, in order to focus on coagulation. As the EL POLY approach for coagulation is stochastic, several computations have been performed. Results are compared to the EE approach in Fig 2. EL POLY introduces

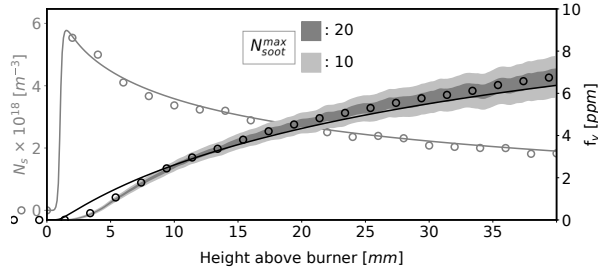


Figure 2: Soot number density (left axis) and soot volume fraction (right axis) for coagulation in the ISF Target Flame 4 (Laminar Premixed Pressurised 2). Comparison between EE (lines) and EL POLY (symbols) with the stochastic noise (shaded area).

a slight stochastic noise on soot volume fraction directly linked to  $N_{soot}^{max}$ . The stochastic noise induced by  $N_{soot}^{max} = 20$  seems reasonable compared to  $N_{soot}^{max} = 10$ . However, near the exit the statistical average of soot volume fraction is slightly higher while the average soot number density is slightly lower. This is due to polydispersity which promotes the coagulation of the largest particles. The number of particles is negatively impacted whereas the soot diameter increases.

## 4. Application to a realistic combustion chamber

### 4.1. Configuration and numerical set-up

The configuration studied in this work is an experimental set-up installed at DLR [33] referred to as ISF-3 Target Flame 1. It is one of the target

pressurized flame within the International Sooting Flame (ISF) workshop. It is designed to study soot formation in gas turbine combustors under elevated pressure, burning ethylene with or without secondary air dilution. The combustor is presented in Fig. 3, also illustrating the flow topology by displaying the instantaneous axial velocity field. The chosen operating point is

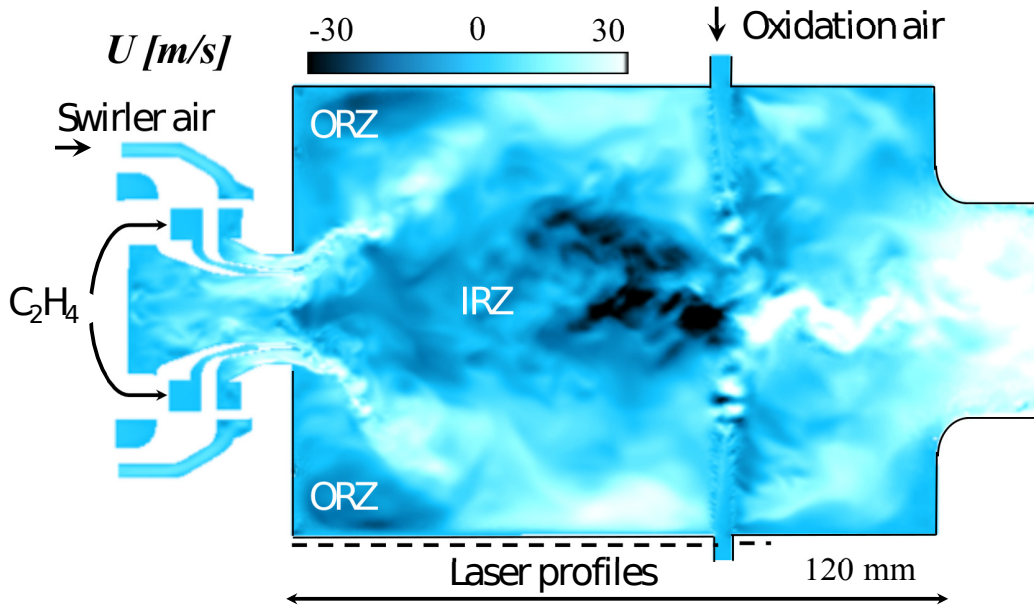


Figure 3: ISF-3 Target Flame 1: Instantaneous axial velocity from LES in a mid-plane cut.

summarized in Table 2. The burner operates under overall lean conditions ( $\phi_{glob} = 0.86$ ) but the primary combustion zone (PZ) is characterized by an overall rich equivalence ratio ( $\phi = 1.2$ ).

The numerical strategy used for the LES of this configuration is fully described and validated in [17]. The domain is discretized into a fully unstructured mesh using 40M tetrahedral elements, and the flow and flame

$\dot{m}_{air}$	$\dot{m}_{air,oxy}$	$\dot{m}_f$	$\phi_{PZ}$
$[kg \cdot s^{-1}]$	$[kg \cdot s^{-1}]$	$[kg \cdot s^{-1}]$	$[-]$
$0.82 \times 10^{-3}$	$4.04 \times 10^{-3}$	$0.86 \times 10^{-3}$	1.2

Table 2: Experimental operating conditions at  $P = 3$  bars [15].

equations are solved with a third order in space and time numerical scheme [34]. The same ARC described in Sec. 3 is employed, associated with the DTFLES turbulent combustion model [35] and the WALE [36] turbulence model. Two simulations including soot, one with EE approach and the other with EL POLY approach were performed for comparison. An instantaneous field of temperature in a mid-cut plane is displayed in Fig. 4(a). As suggested by the white superimposed acetylene isocontour, soot is massively generated in the PZ, downstream the (rich) main flame. The dilution holes are responsible for the temperature decrease along the main axis, visible in Fig. 4(b) where the comparison with experiment shows a very good agreement.

#### 4.2. Soot prediction

Figure 5 presents a qualitative comparison of time-averaged soot mass fraction fields obtained with both formalisms and the experimental results. In both simulations a good order of magnitude and distribution of soot volume fraction is retrieved. The Eulerian and Lagrangian descriptions lead to very similar results, confirming the validity of our Lagrangian particle tracking approach. The different formalisms however lead to slight differences for oxidation. This is due to the removal of particles with a diameter lower than the nuclei ( $=0.98$  nm) in the Lagrangian approach, in order to avoid computing small residual diameter particles, whereas all particles are kept

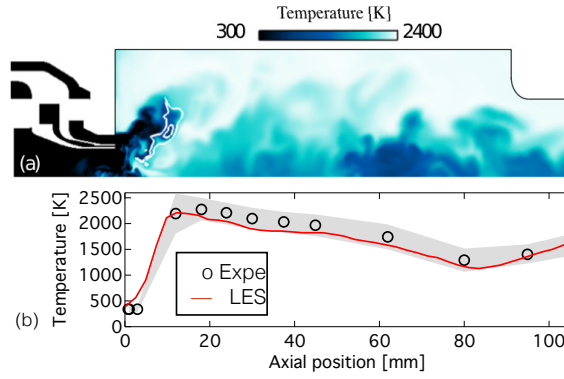


Figure 4: ISF-3 Target Flame 1: (a) Instantaneous temperature field with superimposed acetylene level. (b) Mean axial temperature profile with experimental distribution width (shaded area)

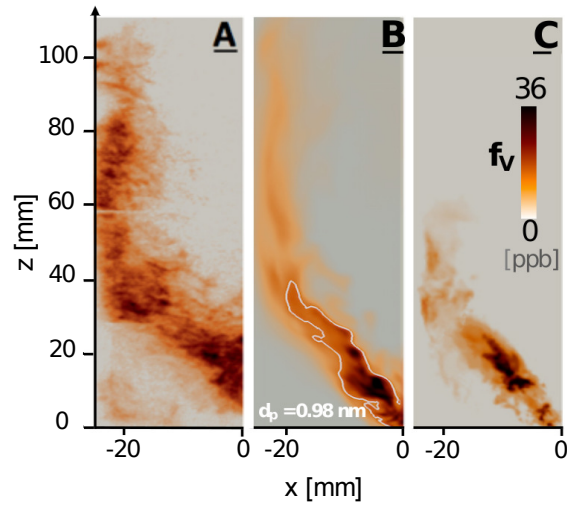


Figure 5: ISF-3 Target Flame 1: Comparison of (A) time-averaged LII soot measurements with time-averaged soot volume fraction from LES using (B) the monodisperse Eulerian (EE) and (C) the polydisperse Lagrangian (EL POLY) approaches. Soot diameter isocontour  $d_p = 0.98 \text{ nm}$  is shown in white.

in the EE approach. A white isocontour of diameter at the nuclei value in Fig. 5b confirms that results for EE and EL POLY are very similar for soot particles larger than nuclei. The main difference between both approaches is the NDF, which is reduced to a Dirac function in the Eulerian approach. Figure 6 shows the instantaneous presence of soot particles (for easier visu-

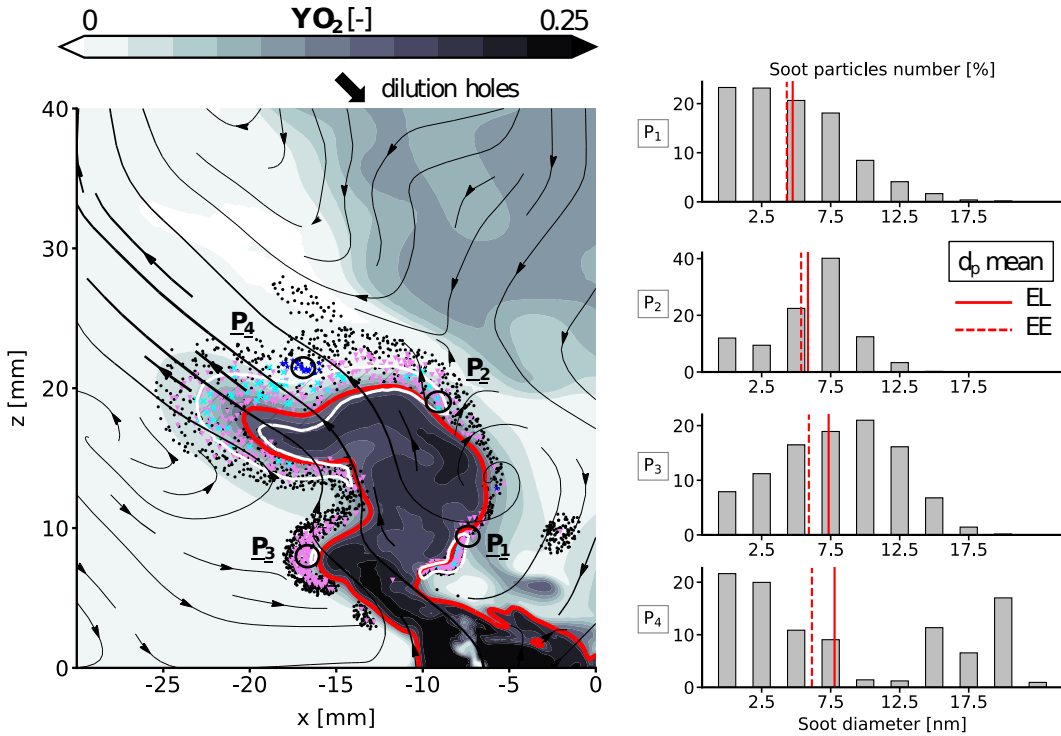


Figure 6: ISF-3 Target Flame 1: Instantaneous soot presence (symbols) in the primary zone with superimposed streamlines,  $O_2$  mass fraction (grey scale), one isocontour of acetylene (white), the isocontour of Temperature at  $T = 1200$  K (red). Four bins of particles are represented: nuclei to 2.5nm ( $\bullet$ ), 2.5 to 7.5 nm ( $\blacktriangledown$ ), 7.5 to 12.5 nm ( $\times$ ) and 12.5 to 20 nm ( $\star$ ). Finally, 4 probes are defined and their respective NDF are shown.

alization only 1 over 100 particles are displayed). Particles are displayed in four bins of size from nuclei size to 20 nm diameter. Streamlines thickened

by the velocity magnitude illustrate the interaction with particle dynamics. The flame position,  $O_2$  and  $C_2H_2$  mass fractions explain why soot remains in the primary zone (Fig. 5). As already seen, soot is formed mainly in post-flame zones rich in  $C_2H_2$ , the soot precursor used in the Leung model. Soot particles are then quickly oxidized although the level of  $O_2$  has significantly decreased in this burnt gas region. Oxidized particles are removed as soon as their size falls below the nuclei size. Only few particles are able to subsist slightly longer downstream until they meet the dilution air jets where they are in turn oxidized. The NDFs obtained with the Lagrangian approach at four probes P1 to P4 represented by large circles on the snapshot are also available in Fig. 6. Although no validation can be made due to the lack of measurement, results demonstrate that the EL POLY approach is capable to describe the NDF with sufficient statistical convergence. The first probe (P1) located in the rich  $C_2H_2$  regions exhibits a single-peak NDF shape due to the strong nucleation in this zone. The bimodality of the soot NDF is retrieved at the forth probe (furthest from the flame) as expected. The comparison of the mean diameter obtained is also plot in Fig. 6 for each probes.

The soot mean diameter follows the same distribution over the four probes for both formalisms. However, the Eulerian mean diameter is lower than the Lagrangian mean diameter, mainly due to the small particles kept in Eulerian and deleted in Lagrangian, in the oxidation zone.

As mentioned in the Introduction, access to the NDF is critical to improve soot modeling. The current results demonstrate that the Lagrangian particle tracking approach is a promising technique to increase the accuracy of soot prediction. This conclusion is re-enforced by the computing times re-

ported in Table 3 for each formalism. Overall the computational time of the Lagrangian approach is of the same order of magnitude than the monodisperse Eulerian approach. This means that the Lagrangian approach gives the NDF at the same computational cost as a monodisperse approach, and allows to envisage sophisticated soot chemistry models in real complex geometries. Note that detailed soot chemistry models may involve additional properties like surface or H/C ratio. If adding such properties is easier with particles than in Eulerian methods [10], it may require more numerical particles to reach sufficient accuracy and then increase the computational cost. However, Table 3 shows that increasing the number of particles will impact the computational cost to a reasonable extent. Another additional complexity will be to include PAH chemistry. This can be achieved either with the use of look-up table [19] or by directly calculating lumped PAHS, as in the 3 sections model of [37]. Both methods induce a low additional cost. All these issues associated to detailed soot chemistry models will be investigated in a future work.

	EE		EL POLY		
$f_s$	-	1	5	1	5
$N_{soot}^{max}$	-	10	10	20	20
<b>CPUh</b>	<b>12500</b>	<b>20250</b>	<b>13600</b>	<b>26650</b>	<b>14675</b>

Table 3: Summary of computational requirements for the computation of 1 *ms* physical time.

## 5. Conclusions

A semi-deterministic Lagrangian particle tracking methodology has been introduced and validated for soot prediction in combustion chambers. Validation on a one-dimensional sooting flame and a gaseous non-premixed burner has been performed by comparison with the original Eulerian Leung model and experiment when available. Results confirm that the approach is suitable for soot modeling and provides accurate results in reasonable computing time. Although further validations are required to assess the accuracy of the predicted NDF, the proposed formalism is ready to include more sophisticated soot models based on more particle properties.

## Acknowledgments

This work was performed using HPC resources from GENCI(Grant A0032B10157): CINES, IDRIS and TGCC. Funding from the European Union within the project SOPRANO (Soot Processes and Radiation in Aeronautical innovative combustion) Horizon 2020 Grant Agreement No. 690724 is gratefully acknowledged.

## References

- [1] M. Shiraiwa, K. Selzle, U. Pöschl, *Free Radical Research* 46 (2012) 927–939.
- [2] B. Zhao, Z. Yang, Z. Li, M. V. Johnston, H. Wang, *Proc. Comb. Inst.* 30 (2005) 1441–1448.
- [3] M. Frenklach, *Chem. Eng. Sci.* 57 (2002) 2229–2239.
- [4] D. L. Marchisio, R. O. Fox, *J. Aerosol Sci.* 36 (2005) 43–73.
- [5] M. E. Mueller, G. Blanquart, H. Pitsch, *Combust. Flame* 156 (2009) 1143–1155.
- [6] M. E. Mueller, H. Pitsch, *Phys. Fluids* 25 (2013).
- [7] P. Rodrigues, B. Franzelli, R. Vicquelin, O. Gicquel, N. Darabiha, *Proc. Combust. Inst.* 36 (2017) 927–934.
- [8] C. Eberle, P. Gerlinger, K. Geigle, M. Aigner, 50th AIAA/ASME/SAE/ASEE Joint Propulsion Conference 2014 (2014) 1–14.
- [9] P. Rodrigues, B. Franzelli, R. Vicquelin, O. Gicquel, N. Darabiha, Accepted in *Combust. Flame* (2017).
- [10] M. Balthasar, M. Kraft, *Combust. Flame* 133 (2003) 289–298.
- [11] M. Lucchesi, A. Abdelgadir, A. Attili, F. Bisetti, *Combust. Flame* 178 (2017) 35–45.

- [12] A. Attili, F. Bisetti, *Computers & Fluids* 84 (2013) 164–175.
- [13] J. C. Ong, K. M. Pang, J. H. Walther, J.-H. Ho, H. K. Ng, *Journal of Aerosol Science* 115 (2018) 70–95.
- [14] K. M. Leung, R. P. Lindstedt, W. P. Jones, *Combust. Flame* 87 (1991) 289–305.
- [15] K. P. Geigle, R. Hadeif, M. Stoehr, W. Meier, *Proc. Comb. Inst.* 000 (2015) 1–8.
- [16] B. Franzelli, E. Riber, B. Cuenot, M. Ihme, In *Proceedings of GT2015, ASME Turbo* (2016) 1–11.
- [17] A. Felden, E. Riber, B. Cuenot, *Combust. Flame* 191 (2018) 270–286.
- [18] M. E. Mueller, G. Blanquart, H. Pitsch, *Proceedings of the Combustion Institute* 32 I (2009) 785–792.
- [19] G. Lecocq, D. Poitou, I. Hernández, F. Duchaine, E. Riber, B. Cuenot, *Flow Turb. and Combustion* 92 (2014) 947–970.
- [20] J. Y. Hwang, S. H. Chung, *Combust. Flame* 125 (2001) 752–762.
- [21] X. Hao, H. Zhao, Z. Xu, C. Zheng, *Aerosol Sci. Tech.* 47 (2013) 1125–1133.
- [22] J. Wei, F. E. Kruijs, *Chemical Eng. Sc.* 104 (2013) 451–459.
- [23] A. Khadilkar, P. L. Rozelle, S. V. Pisupati, *Powder Technology* 264 (2014) 216–228.

- [24] F. E. Kruis, A. Maisels, H. Fissan, *AIChE Journal* 46 (2000) 1735–1742.
- [25] A. L. Garcia, C. Van Den Broeck, M. Aertsens, R. Serneels, *Physica A Statistical Mechanics & Its Applications* (1987) 535–546.
- [26] G. Kotalczyk, F. E. Kruis, *J. Comput. Phys.* 340 (2017) 276–296.
- [27] Z. Xu, H. Zhao, C. Zheng, *J. Comput. Phys.* 281 (2015) 844–863.
- [28] K. Liffman, *J. Comput. Phys.* 100 (1992) 116–127.
- [29] M. Smith, T. Matsoukas, *Chem. Eng. Sci.* 53 (1998) 1777–1786.
- [30] Y. Lin, K. Lee, T. Matsoukas, *Chem. Eng. Sci.* 57 (2002) 2241–2252.
- [31] W. J. Menz, J. Akroyd, M. Kraft, *J. Comput. Phys.* 256 (2014) 615–629.
- [32] M. Tsurikov, K. P. Geigle, V. Krüger, Y. Schneider-Kühnle, W. Stricker, R. Lückcrath, R. Hedef, M. Aigner, *Combust. Sc. Tech.* 177 (2005) 1835–1862.
- [33] K. P. Geigle, R. Hedef, W. Meier, *J. Eng. Gas Turb. and Power* 136 (2014) 021505.
- [34] O. Colin, M. Rudgyard, *J. Comput. Phys.* 162 (2000) 338–371.
- [35] O. Colin, F. Ducros, D. Veynante, T. Poinso, *Phys. Fluids* 12 (2000) 1843–1863.
- [36] F. Nicoud, F. Ducros, *Flow, Turb. Combust.* 62 (1999) 183–200.
- [37] C. Eberle, P. Gerlinger, M. Aigner, *Combust. Flame* 179 (2017) 63–73.